Efficient sub-Doppler laser cooling of an Indium atomic beam

Jae-Ihn Kim,[*] **Dietmar Haubrich, and Dieter Meschede**

Institut für Angewandte Physik, Universität Bonn, Wegelerstraße 8, 53115 Bonn, Germany

[*]*kim@iap.uni-bonn.de*

Abstract: We have realized efficient transverse cooling of an Indium atomic beam by combining optical pumping with a closed cycle UV laser cooling transition at 325.6 nm. The transverse velocity of the atomic beam is reduced to 13.5 ± 3.8 cm/s, well below the Doppler cooling limit. The fraction of laser-cooled In atoms is enhanced to 12 ± 3 % by optical pumping in the present experiment. It can be scaled up to approach 100% efficiency in cooling, providing high brightness atomic beams for further applications. Our results establish In on the map of elements suitable for applications involving laser cooling.

© 2009 Optical Society of America

References and links

1. J. J. McClelland, R. E. Scholten, E. C. Palm, and R. Celotta, "Laser-focused atomic deposition," Science **262**, 877–880 (1993).
2. D. Meschede and H. Metcalf, "Atomic nanofabrication: atomic deposition and lithography by laser and magnetic forces," J. Phys. D **36,** R17–38 (2003).
3. Th. Schulze, T. Müther, D. Jürgens, B. Brezger. M. K. Oberthaler, T. Pfau, and J. Mlynek, "Structured doping with light forces," Appl. Phys. Lett. **78**, 1781–1783 (2001).
4. S. Kuhr, W. Alt, D. Schrader, M. Müller, V. Gomer, and D. Meschede, "Deterministic delivery of a single atom," Science **293**, 278–280 (2001).
5. S. B. Hill and J. J. McClelland, "Atoms on demand: Fast, deterministic production of single Cr atoms," Appl. Phys. Lett. **82**, 3128–3130 (2003).
6. R. E. Scholten, R. Gupta, J. J. McClelland, R. J. Celotta M. S. Levenson and M. G. Vangel, "Laser collimation of a chromium beam," Phys. Rev. A **55**, 1331–1338 (1997)
7. G. Uhlenberg and J. Dirscherl and H. Walther, "Magneto-optical trapping of silver atoms," Phys. Rev. A **62**, 063404 (2000)
8. B. Smeets, R. W. Herfst, L. P. Maguire, E. te Sligte, P. van der Straten, H. C. W. Beijerinck and K. A. H. van Leeuwen, "Laser collimation of an Fe atomic beam on a leaky transition," Appl. Phys. B **8**0, (2005) 833
9. M. Watanabe, R. Ohmukai, U. Tanaka, K. Hayasaka, H. Imajo, and S. Urabe, "Velocity control of an Yb beam by a frequency-doubled mode-locked laser," J. Opt. Soc. Am. B 13, 2377–2381 (1996)
10. J. J. McClelland, and J. L. Hanssen, "Laser cooling without repumping: a magneto-optical trap for erbium atoms," Phys. Rev. Lett. **9**6, 143005 (2006)
11. R. W. McGowan, D. M. Giltner, and S. A. Lee, "Light force cooling, focusing, and nanometer-scale deposition of aluminum atoms," Opt. Lett. **20**, 2535–2537 (1995).
12. B. Klöter, C. Weber, D. Haubrich, D. Meschede, and H. Metcalf, "Laser cooling of an indium atomic beam enabled by magnetic fields," Phys. Rev. A **77**, 033402 (2008).
13. S. J. Rehse, K. M. Bockel, and S. A. Lee, "Laser collimation of an atomic gallium beam," Phys. Rev. A **69**, 063404 (2004).
14. P. Zimmermann, "Level-Crossing-Experimente zur Untersuchung der Hyperfeinstruktur des $5d^2D_{5/2}$-Terms im Indium I-Spektrum," Z. Physik A, **233**, 21–26 (1970).
15. U. Rasbach, J. Wang, R. dela Torre, V. Leung, B. Klöter, D. Meschede, T. Varzhapertyan and D. Sarkisyan, "One- and two-color laser spectroscopy of indium vapor in an all-sapphire cell," Phys. Rev. A **70**, 033810, (2004).

16. J. I. Kim and D. Meschede, "Continuous-wave coherent ultraviolet source at 326 nm based on frequency tripling of fiber amplifiers," Opt. Express **16**, 10803–10808 (2008).
17. J. Dalibard and C. Cohen-Tannoudji, "Laser cooling below the Doppler limit by polarization gradients: simple theoretical models," J. Opt. Soc. Am. B **6**, 2023–2045 (1989).
18. F. Röser, C. Jauregui, J. Limpert, and A. Tünnermann, "94 W 980 nm high brightness Yb-doped fiber laser," Opt. Express **16**, 17310–17318 (2008).

1. Introduction

Laser cooled atomic gases and atomic beams are widely studied samples in experimental research in atomic and optical physics. For the application of ultra cold gases as model systems for e.g. quantum many particle systems, the atomic species is not very important. Thus this field is dominated by alkaline and earthalkaline elements which are easily accessible with conventional laser sources and have convenient closed cooling transition. On the other hand, laser cooled atoms may also be interesting for technological applications, for instance for the creation of novel materials by atomic nanofabrication (ANF) [1, 2]. There it will be important to use technologically relevant materials. As an example, using group III atoms of the periodical table in ANF may open a route to generate fully 3D structured composite materials [3].

For e.g. a successful ANF experiment a transversely laser-cooled atomic beam is essential because the atomic beam collimation plays a critical role in the quality of structures (e.g. contrast, sharpness) produced by ANF methods and, equally important, enhances atomic beam flux to reduce the deposition time [2]. Furthermore, laser cooling of group III atoms allows the first step towards precision manipulation of technologically preferred materials in the single atom basis [4, 5].

Atomic species applicable in laser cooling but other than alkaline, earthalkaline, and noble gas elements are still scarce: Cr [6], Ag [7], Fe [8], Yb [9], Er [10], and group III elements Al [11], In [12], Ga [13]. For these elements, optical transitions accessible with conventional laser sources exist and have been applied. Laser cooling is most efficient for truly closed cycling transitions, since even small leaks at the per mil level may render the cooling process inefficient. For group III elements, a closed system is indeed offered with the $^2P_{3/2} \rightarrow \,^2D_{5/2}$ cycling transition. Experimental realization, however, is challenged by the fact that the elevated $^2P_{3/2}$ state has small thermal population and the transition wavelengths are in the UV already. For Al and Ga, laser cooling on this transition has been demonstrated [11, 13], but only for the small thermal population of the $^2P_{3/2}$ state. As an alternative we have previously studied two-color laser cooling of Indium involving both the $^2P_{1/2}$ and $^2P_{3/2}$ ground states but found that the complicated level scheme involving coherent phenomena such as dark states impaired the efficient and robust application of this scheme for laser cooling [12].

In this paper we now present a scheme that overcomes the drawbacks of previous attempts: Transverse laser cooling of an Indium atomic beam is realized with the closed cycling transition in analogy with Al and Ga. The UV light required for this application is generated with robust diode and fiber-based light sources. In addition, the total fraction of laser cooled atoms is significantly enhanced by optically pumping atoms into the $^2P_{3/2}$ lower level of the cooling transition.

2. Experiments and results

Indium has two isotopes, ^{113}In and ^{115}In, with an abundance of 4.3 % and 95.7 %, respectively. Both isotopes have the same nuclear spin 9/2. Fig. 1 shows the relevant atomic levels of ^{115}In including hyperfine structure [14]. The $^2P_{1/2}, F = 4,5 \rightarrow \,^2S_{1/2}, F' = 5$ transitions at $\lambda_{\text{pump}} = 410$ nm are used for optical population pumping, the $^2P_{3/2}, F'' = 6 \rightarrow \,^2S_{1/2}, F' = 5$ at $\lambda_{\text{probe}} = 451$ nm serves as a probe transition. The UV cycling transition is realized in our experiments

using the hyperfine transition $^2P_{3/2}$, $F'' = 6 \rightarrow {}^2D_{5/2}$, $F''' = 7$ at $\lambda_{\text{cool}} = 325.6$ nm.
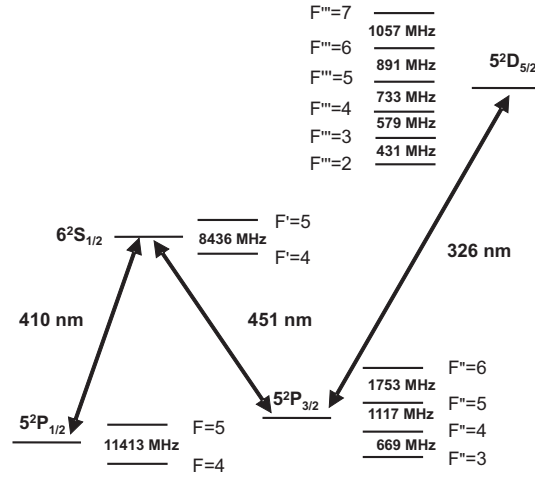

Fig. 1. Energy level scheme of ^{115}In including hyperfine structures [14]. The cycling transition for laser cooling, $^2P_{3/2}, F'' = 6 \rightarrow {}^2D_{5/2}, F''' = 7$, is driven by UV light at $\lambda_{\text{cool}} = 325.6$ nm.

Table 1. Atomic parameters of the cooling transition $^2P_{3/2}$, $F'' = 6 \rightarrow {}^2D_{5/2}$, $F''' = 7$.

Parameter		Value
Wavelength	λ_{cool}	325.6 nm
Life time $^2D_{5/2}$	τ	7.7 ns
Decay rate $^2D_{5/2}$	$\Gamma/2\pi$	20.7 MHz
Recoil velocity	$v_{\text{r}} \equiv \hbar k/M$	1.1 cm/s
Doppler capture velocity	$v_{\text{c}} \equiv \Gamma/k$	6.7 m/s
Velocity at Doppler limit	$v_{\text{D}} \equiv \sqrt{\frac{\hbar\Gamma}{2M}}$	19 cm/s
Saturation intensity	$I_{\text{sat}} \equiv \frac{hc\pi\Gamma}{3\lambda_{\text{cool}}^3}$	78 mW/cm^2

The experimental arrangement is illustrated in Fig. 2. An In atomic beam is produced by a commercial effusion cell. A crucible containing In is resistively heated up to 1200 °C. The thermal fraction of In atoms in the $^2P_{3/2}$, $F'' = 6$ state is 7 %. The most probable longitudinal velocity is measured to be 560 m/s. The atomic beam is pre-collimated by a mechanical aperture with 0.5 mm diameter yielding 3 mrad initial divergence.

In order to enhance the population in the ground state of the cooling transition the Indium atoms are optically pumped to the $^2P_{3/2}$ state by violet pump beams at λ_{pump}. Two external cavity diode lasers produce 4 mW for the $4 \rightarrow 5$ and 2 mW for the $5 \rightarrow 5$ hyperfine transition. They are frequency locked to the center of Doppler-free saturated absorption lines using an all-sapphire cell [15]. The beams are superposed by a polarizing beam splitter cube and sent to the atomic beam with cross section 1 mm × 2 mm in the pumping region. With this method the fraction of In atoms in the $^2P_{3/2}$, $F'' = 6$ lower cooling level is enhanced by a factor of up to 7 corresponding to 50 % of the atoms in the ground state of the cooling transition.

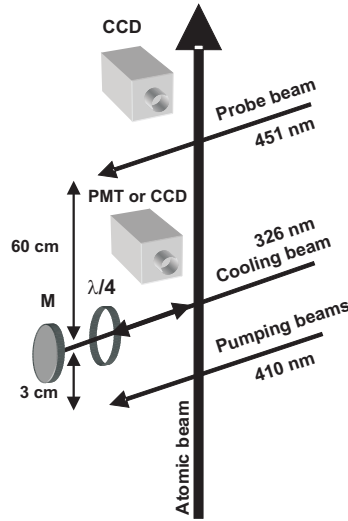In the cooling region, 3 cm above the pumping region, the UV light beams interact at

Fig. 2. Schematic of the experimental setup. The atoms are optically pumped to the $^2P_{3/2}$ levels by two violet lasers at λ_{pump} in the pumping region. In the cooling region, UV light at λ_{cool} is applied with a polarization gradient configuration (lin $\perp$ lin) for laser cooling. The spatial distribution of the atomic flux density is measured by exciting the atoms at λ_{probe} and imaging the fluorescence distribution at λ_{pump} in the probe region.

right angles with the atomic beam. A weak magnetic guiding field (2 G) is applied in the direction of the cooling laser beam. The cooling laser light at λ_{cool} is generated by upconversion of the output of two fiber amplifiers driven by a single diode laser at 3 λ_{cool} [16]. A frequency doubling stage with a critically phase-matched KNbO$_3$ crystal is employed (3 $\lambda_{\text{cool}} \rightarrow 3\ \lambda_{\text{cool}}/2$), and summation is achieved with a BBO crystal in a doubly resonant cavity ($(3\ \lambda_{\text{cool}})^{-1} + (3\ \lambda_{\text{cool}}/2)^{-1} \rightarrow \lambda_{\text{cool}}^{-1}$). The UV output light of the summation stage is collimated by a pair of cylindrical lenses yielding a cross section of 1 mm $\times$ 3 mm with 7 mW of UV power and corresponding to a saturation parameter ($s = I/I_{\text{sat}} = 4$). The 3 mm interaction length with the atomic beam corresponds to an average interaction time of $\tau_{\text{int}} = 700\ \tau$.

Laser-induced UV fluorescence in the cooling region is detected by a photo-multiplier tube and used to control the laser frequency. Fig. 3(a) shows a fluorescence spectrum (solid line) along with a Doppler limited In absorption spectrum (dotted line) from a hollow cathode lamp for comparison. The FWHM of the $6 \rightarrow 7$ cooling transition is measured to be about 44 MHz with contributions by atomic beam divergence (5 MHz), power broadening (27 MHz, $s = 0.7$), and laser spectral line width (30 MHz). The small discrepancy between the measured and expected widths can be traced to the uncertainty in the frequency calibration caused by the nonlinearity of a PZT used for frequency tuning of diode laser. Note that the frequency stability requirements for the laser sources are moderate and can be realized with simple control techniques. In the cooling and heating experiment, the UV laser frequency is side-locked to one of the slopes of the fluorescence signal of the cycling transition induced by cooling laser beam ($s = 4$) yielding an appropriate detuning of $\sim -\Gamma$ for cooling and $\sim +\Gamma$ for heating.

In order to induce a lin $\perp$ lin polarization gradient in the cooling region a linearly polarized beam is sent to the atomic beam and retro reflected passing a quarter wave plate twice which causes a 90° rotation of the polarization. The propagation directions of the cooling beams are set at right angles to the atomic beam within 2 mrad uncertainty by measuring the fluorescence induced by the overlapped counter propagating UV beams with a photomultiplier tube. Scan-
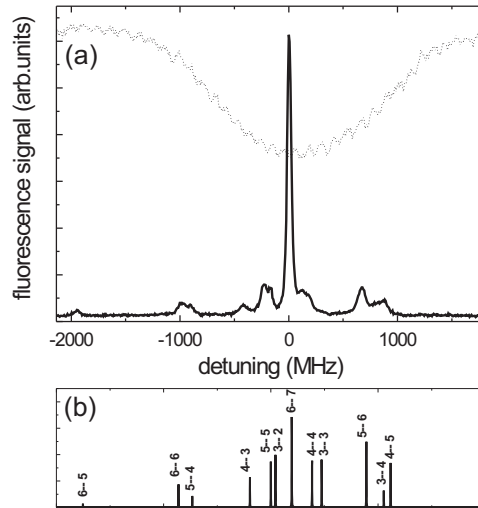
Fig. 3. (a) Solid line: Fluorescence spectrum of the In $^2P_{3/2} \to\ ^2D_{5/2}$ transitions induced by the UV laser at λ_{cool}. Dotted line: Doppler limited absorption spectrum of a hollow cathode lamp. The frequency of the laser is calibrated by the separation between $6 \to 5$ and $6 \to 7$ transitions (1948 MHz). The FWHM of the peak of the $6 \to 7$ transition is 44 MHz. (b) Theoretical spectrum indicating position and oscillator strengths of hyperfine transitions. In the observed spectrum, optical cycling leads to strong enhancement on the closed $6 \to 7$ transition.

ning the laser frequency across the resonance then produces a Doppler sensitive signal with two maxima symmetric to the undisturbed atomic resonance when the two counter propagating beams are not aligned perpendicularly with respect to the atomic beam. Atomic parameters of the In atom are summarized in Tab. 1.

A free-flight section of $l = 60$ cm takes the atomic beam from the cooling to the probe region. Here, the transverse beam profile is measured by laser-induced fluorescence imaged with a CCD camera. The probe beam at λ_{probe} is generated by a frequency-doubled Ti:sapphire laser whose frequency is locked to a temperature-stabilized reference resonator. An output power of 0.5 mW is obtained after single-pass frequency doubling of the infrared beam at 902 nm by a periodically-poled KTP crystal. Since on excitation by the probe laser in the open $^2P_{3/2} \to\ ^2S_{1/2}$ transition every atom undergoes 1.2 fluorescence cycles on average only the fluorescence distribution is directly proportional to the atomic flux density.

Efficient sub-Doppler laser cooling caused by polarization gradient cooling [17] for red detuned cooling laser beams as well as heating effects for blue detuned laser beams are observed by flux enhancements and attenuations in the probe region as shown in Fig. 4. The insets of Fig. 4(a) show fluorescence images of the In atomic beam with a striking bright region of cooled atoms (left, red detuned cooling laser), and a dark region caused by the expulsion of heated atoms (right, blue detuned cooling laser).

For further analysis the fluorescence images are integrated along the direction transverse to the propagation direction of the cooling laser. Fig. 4(a) shows the profiles of the laser-cooled (solid line), the uncooled (dotted line), and the heated (dashed line) atomic In beam from a partially clogged aperture in the probe region, respectively. Here, the FWHM of the cooled fraction
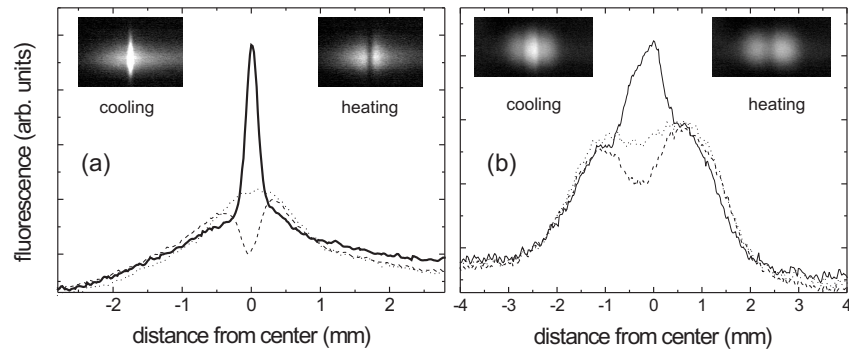
Fig. 4. Integrated transverse profiles of the atomic beam from (a) the partially clogged aperture and (b) the cleaned aperture in the probe region: (solid line) cooling with the lin $\perp$ lin polarization gradient ($\Delta \sim - \Gamma$), (dotted line) no laser cooling, (dashed line) heating with lin $\perp$ lin polarization gradient ($\Delta \sim + \Gamma$). Insets: Images of a cooled (left) and a heated (right) In atomic beam. In the measurement for Fig. 4(b), the cooling laser power is reduced to about 2/3 of the initial power due to a technical problem.

is measured to be 0.2 mm, which is smaller than the nominal initial width of the atomic beam (0.5 mm). This could be attributed to the fact that residual In partially clogged the mechanical aperture so that the effective diameter of the aperture was decreased. After cleaning the aperture, we have re-measured the FWHM of the laser-cooled atomic beam to be 0.86 ± 0.07 mm yielding the 13.5 ± 3.8 cm/s transverse velocity well below the Doppler limited velocity of 19 cm/s as shown in Fig. 4(b). The corresponding full divergence is 0.48 ± 0.13 mrad. In this measurement, the maximum cooling laser power was reduced to 2/3 of the initial laser power ($s = 3$) by a technical problem (burning damage of the Yb-doped fiber). We attribute the reduction of the laser cooling and heating effects in Fig. 4(b) compared to Fig. 4(a) to the deteriorated laser power.

The fraction of laser-cooled atoms is deduced to be 12 ± 3 % from the integrated atomic beam profile. It is currently limited by the number of effective scattering events which is deduced by analyzing the laser-heated profiles to be 50 for the most probable longitudinal velocity of 560 m/s. The asymmetry in the laser cooled beam profile could be attributed to an imbalance in the cooling laser power induced by the uncoated vacuum windows. After interaction of the In atoms with the cooling laser, most of the In atoms (> 99 % deduced by comparing the area of each atomic beam profile) survive within the cooling transition indicating no significant leakage in the cycling transition.

3. Conclusion

In summary, we have realized an experiment showing efficient sub-Doppler laser cooling of an In atomic beam on a cycling transition. The fraction of In atoms in the ground state of the cycling transition was enhanced by optical pumping. The fraction of laser-cooled In atoms can be further enhanced by increasing the number of scattering events, i.e. increasing the interaction length and the cooling laser power in order to extend the velocity range captured by Doppler cooling processes. Realistic improvements include higher UV power (100 mW instead of 7 mW) [16, 18], longer interaction length (10 mm instead of 3 mm) and additional optical pumping frequencies driving $^2P_{3/2}$, $F'' = 4, 5 \rightarrow {}^2S_{1/2}$, $F' = 5$ transitions at λ_{probe}. With these advances one may well approach 100 % efficiency in laser cooling of In atomic beams.